LAWRENCE
LIVERMORE
NATIONAL
LABORATORY

LLNL-TR-739837

FY17 NIF Performance Quad Campaign: laser performance results and conclusions

J. M. Di Nicola, G. Mennerat, G. Widmayer

October 11, 2017

Disclaimer

This work performed under the auspices of the U.S. Department of Energy by Lawrence Livermore National Laboratory under Contract DE-AC52-07NA27344.

Mail Station: L-462
Ext: 2-4877

Date 9-28-2017

TO: Paul Wegner

FROM: J. M. Di Nicola, G. Mennerat, C. Widmayer

SUBJECT: FY17 NIF Performance Quad Campaign: laser performance results and conclusions

1. Executive Summary

The FY17 NIF Performance Quad Campaign exercised a single quad of NIF (Q45T) at elevated energy to assess the impact of recent improvements to the infrared (1ω) and ultraviolet (3ω) section of the laser on integrated performance [1,2,3]. The campaign employed ignition-relevant hydro-scaled versions of high-foot pulses with energy up to 13.5 kJ / 2.5 TW at 3ω per beamline, equivalent to 2.6 MJ / 480 TW for full-NIF operations. The main objectives were 1) an updated assessment of laser performance limits with validation of laser simulation codes, and 2) extension of 3ω optics lifetime models to higher fluence to estimate the cost of operating NIF at increased energy. This report summarizes the laser performance results of the campaign. The optics performance results are described in a companion document [4].

The campaign comprised a total of 25 full-system shots: 8 to ramp up and prepare the 1ω Main Laser, followed by 17 shots to Target Chamber Center (TCC), including 5 shots to condition the transport mirrors and final optics up to elevated energy, then 6 shots at elevated energy interleaved with 6 low-energy optics "cleaning shots". A shot summary table is provided at the end of this report.

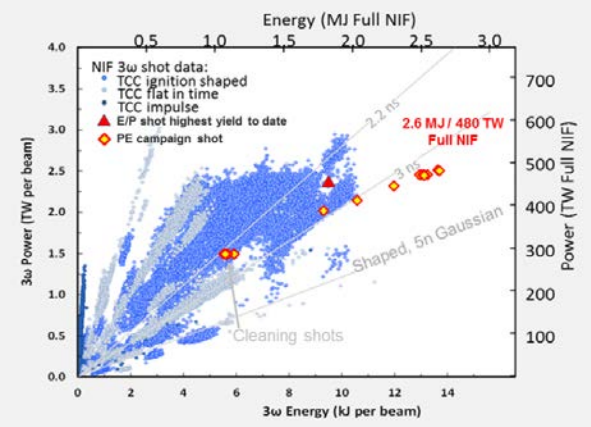

Figure 1: NIF energy-power diagram. Past shots are in blue, Performance Quad shots are the yellow diamonds.

The campaign met its laser performance objectives. Ignition-quality pulses were successfully delivered to TCC up to a 3ω quad energy and power of 54.6 kJ, 9.9 TW. The 1ω and 3ω laser performance measured at the outputs of the Main Laser and Final Optics Assembly were both consistent with the modeled expectations for energy, power, and near field beam quality to within a few percent. On the highest energy/power shots, a small amount of filamentary damage from B-integral-induced self-focusing was observed on three of the four beams in the quad. The damage occurred in a thin (~3-mm wide) strip on the thick side of the Wedged Focus Lenses (WFLs), and is strongly correlated with an intensification at the edge of the beam profile exhibited in the 3ω near-field fluence data. Virtual Beam Line (VBL) simulations have been able to reproduce the observed edge intensification, but as yet do not predict that filamentation should have occurred. Resolving this discrepancy is a topic for future work, along with identifying ways to

increase power limits and margin against filamentation. For example, simulations suggest that it is possible to mitigate the intensification of the beam edge by installing a softer-edged serrated apodizer in the front end.

2. 1ω Performance

The 1ω Main Laser performed according to expectations. Beam quality was excellent and the delivered performance was consistent with the requested performance up to 22.5 kJ per beam, the maximum tested. Agreement between delivered energy and requested energy was better than 2%. The agreement between delivered and requested power was in the range of that required for ignition experiments (Figure 2).

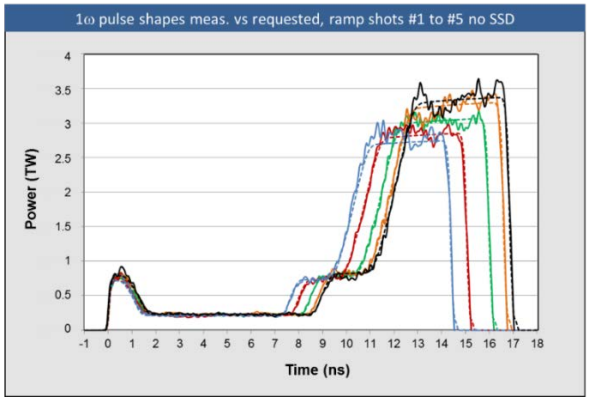

Figure 2: 1ω pulse shapes from B454 measured at the output of the Main Laser (solid lines), compared to request (dashed lines). Colors correspond to Full-NIF-Equivalent 3ω energies of 2.0 MJ (blue), 2.2 MJ, 2.4 MJ, 2.5 MJ, and 2.6 MJ (black).

An example comparison of modeled to measured 1ω performance is shown in Figure 3, demonstrating the high degree to which the models have been validated. A small adjustment of the laser amplification saturation fluence in the beam 454 model was required to better match the measured temporal pulse profiles. After this adjustment, the overall agreement with the measurements at elevated energy was better than 1.3% for the energy, and better than 5% for the time-resolved power with 1 ns boxcar smoothing (for the two beams that were equipped with 1ω power sensors: B451 and B454). Additionally, prior to the campaign an improved method was implemented for computing the 2D-resolved small signal gain in the context of beam multiplexing and vignetting in the Main Amplifiers. The new method resulted in better qualitative and quantitative agreement with the measured near field fluence profiles, in particular the low-frequency components of the profiles.

Energetics 1ω

Beam	OSP req. (kJ)	OSP meas. (kJ)	Diff (%)
B451	20.89	20.75	-0.7
B452	20.42	20.32	-0.5
B453	19.81	19.73	-0.4
B454	20.89	20.62	-1.3

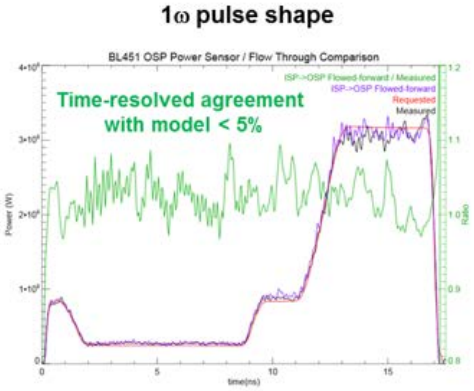

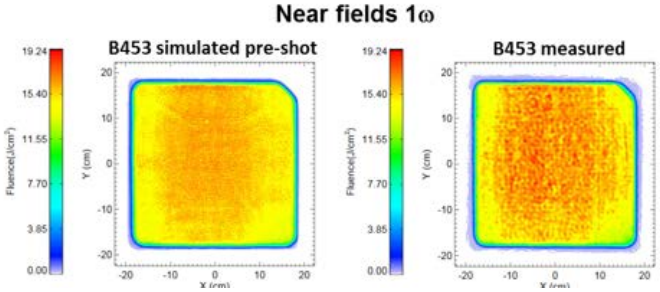

Figure 3: Overall agreement between measurements and the models at high-energy.

Achieving and maintaining good spatial beam quality was an important part of this campaign. Each preamplifier module in the NIF front-end is equipped with a Programmable Spatial Shaper (PSS) system containing an optically-addressed liquid-crystal light-valve. The PSS is used to sculpt the spatial fluence profile injected into the four beams in each quad to serve two specific functions. One is to flatten the output beam profile by pre-compensating for the laser gain spatial nonuniformity in the flash-lamp-pumped main amplifiers (referred to as PSS beam flattening). The optimum transmission map for the PSS is derived from the near-field fluence profiles measured at the output of the Main Laser on low-energy (unsaturated) shots. When this optimum transmission map is applied, the output beam quality (fluence contrast) is improved by ~2x at low energy (Figure 4, top row).

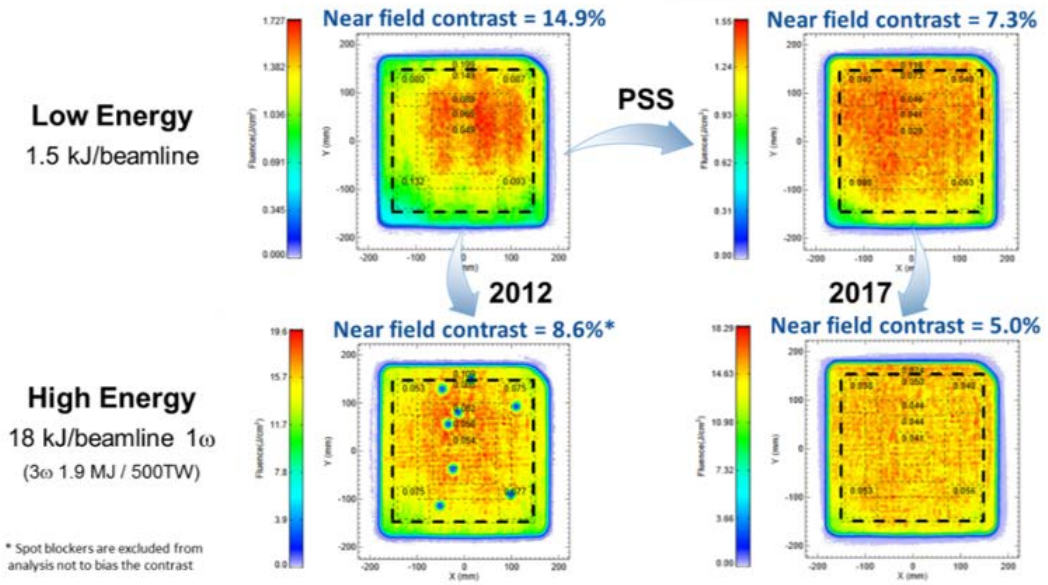

Figure 4: Examples of near-field beam quality obtained on beam B454 with (right) and without (left) PSS beam flattening. Top and bottom rows show low and high energy operation, respectively

The same optimum transmission map also improves beam quality at high energy. Figure 4 (bottom row) compares the B454 near-field fluence profile measured during the 1ω energy ramp portion of the campaign (shot N161115-001-999) with the measured fluence profile from the same beam on shot N120705-002-999, taken at similar energy and power but without PSS beam flattening. In this case the fluence contrast was reduced from 8.6% to 5%. More generally, the contrast at the output of the main laser was improved from 8-9% to 5-6% on average for the quad, and maintained at this level for the duration of the campaign (Figure 5).

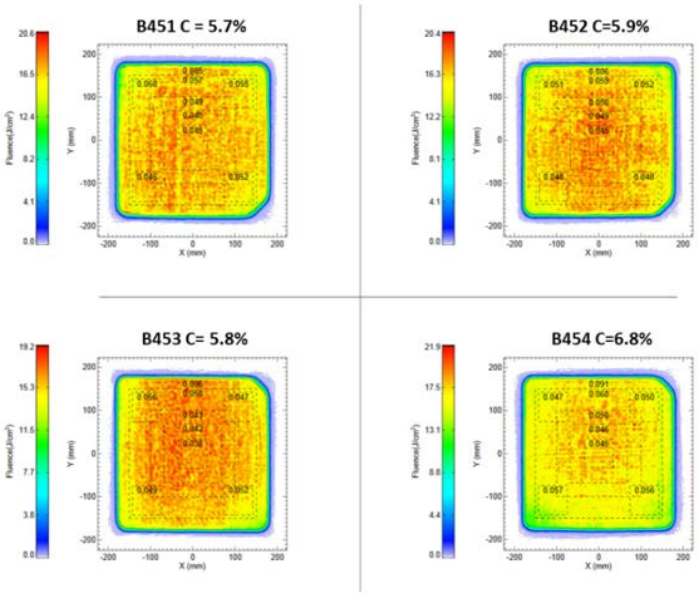

Figure 5: Measured 1ω near-field fluence profiles at the output of the Main Laser for the four beams of Q45T on shot N170309-001-999 (2.6 MJ 3ω at TCC Full NIF Equivalent)

The effect of the reduced fluence contrast is to significantly reduce the high-fluence tails of the near-field fluence distribution, even at large saturation. For example, the fraction of energy above 17 J/cm^2 in an 18 kJ beam was reduced by ~100x when the PSS was applied (Figure 6). This level of improvement and its impact on 3ω optics operating cost were the major drivers behind the implementation of PSS beam flattening in late 2015 [5], and were included in the models and simulations during the planning for this campaign.

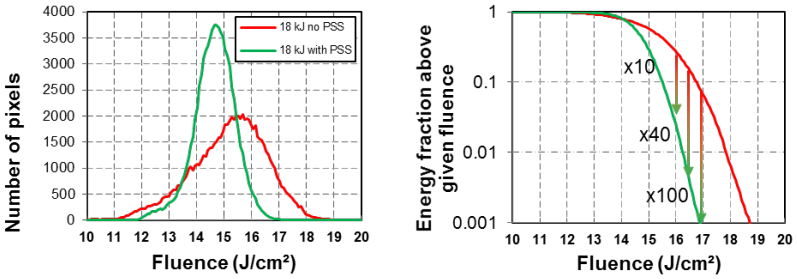

Figure 6: Measured 1ω near-field fluence histograms at the output of the Main Laser with PSS beam flattening (green) and without PSS beam flattening (red).

A second important function of the PSS is to create shadows ("spot blockers") at specific locations in the beam to mask defects or damage spots in the final optics. The spot blocker is designed to have the minimum diameter and edge width that produces acceptable modulation at out-of-relay-plane components when the effects of diffraction, spatial filtering and B-integral are properly accounted for. The diameter and edge width of the spot blockers had been optimized to 2.2 cm FWHM and 2.2 cm respectively for NIF energies up to 1.9 MJ. The increased level of amplifier saturation and total system B-integral associated with higher energy operation changes this optimum, requiring larger spot blockers to maintain the same machine safety margins. VBL simulations determined that a diameter of 2.6 cm for the spot blockers was this new optimum.

The new spot blocker specifications were verified by performing shots to the output of the Main Laser corresponding to 1.8 and 2.6 MJ 3ω TCC Full NIF Equivalent, with the Output Sensor Package (OSP) near-field camera imaged at SF4 - the optical component furthest out of relay. The comparison of the images and the spot blocker profiles (Figure 7) demonstrates machine safety margin similar to the 1.8 MJ nominal case when 2.6 cm spot blockers are operated at 2.6 MJ.

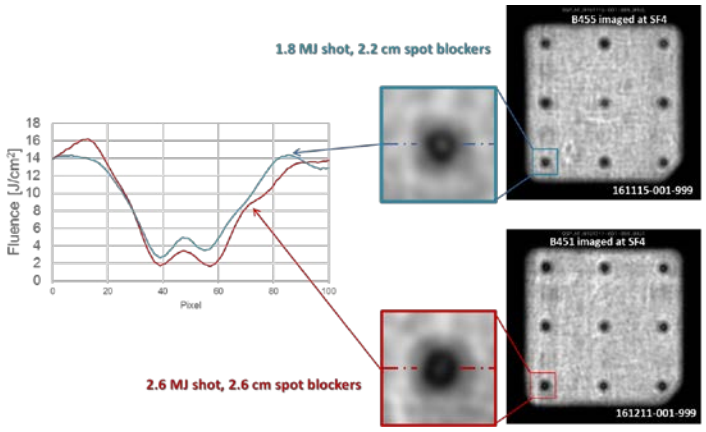

Figure 3: Spot blocker profiles measured at the equivalent plane of SF4 for 1.8 MJ 3ω TCC Full NIF Equivalent shot with 2.2 cm spot blockers (top, blue) and 2.6 MJ 3ω TCC Full NIF Equivalent shot with 2.6 cm spot blockers (bottom, red). Lineouts (left) through the spot blocker profiles shows similar shape and modulation level.

3. 3ω Performance

The 3ω laser performance met all requirements for energy and power. As shown in Figure 8, all shots at elevated energy were delivered within 2% of the request. To save time, the rules of engagement for front end energy tolerance were relaxed on the 1.1 MJ cleaning shots, resulting in a larger variability between the requested and delivered energy on these shots.

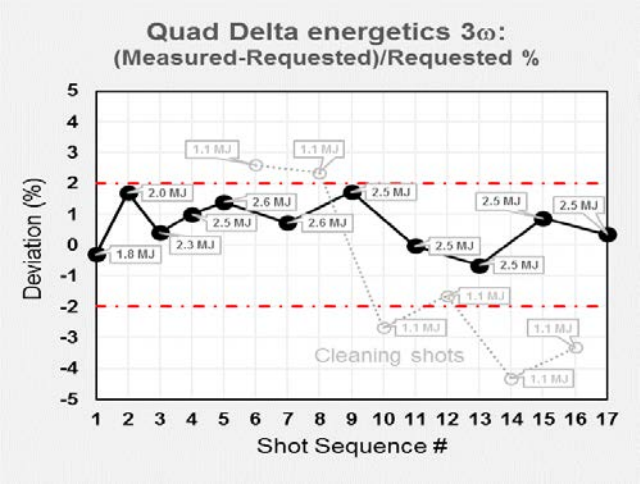

Figure 8: Energy delivery accuracy for high energy shots (dark symbols) and low energy cleaning shots (light symbols). Labeled energies are 3ω TCC Full NIF Equivalent.

The final shot in the 3ω energy ramp sequence (#5) culminated with a total 3ω quad energy of 54.61 kJ delivered to TCC, within 1.4% of the requested energy. The power at 3ω was also delivered within the accuracy currently supported for ignition experiments. As described in [2], two of the beams in the quad were equipped with 3ω power sensors for this campaign. The time-resolved quality of the 3ω model (the comparison between the 3ω power measured on these two beams and the 3ω power inferred from the 1ω power measured at the output of the Main Laser and flowed-forward by model) are within 5% for most of the time epochs during the pulse (right hand plots, Figure 9).

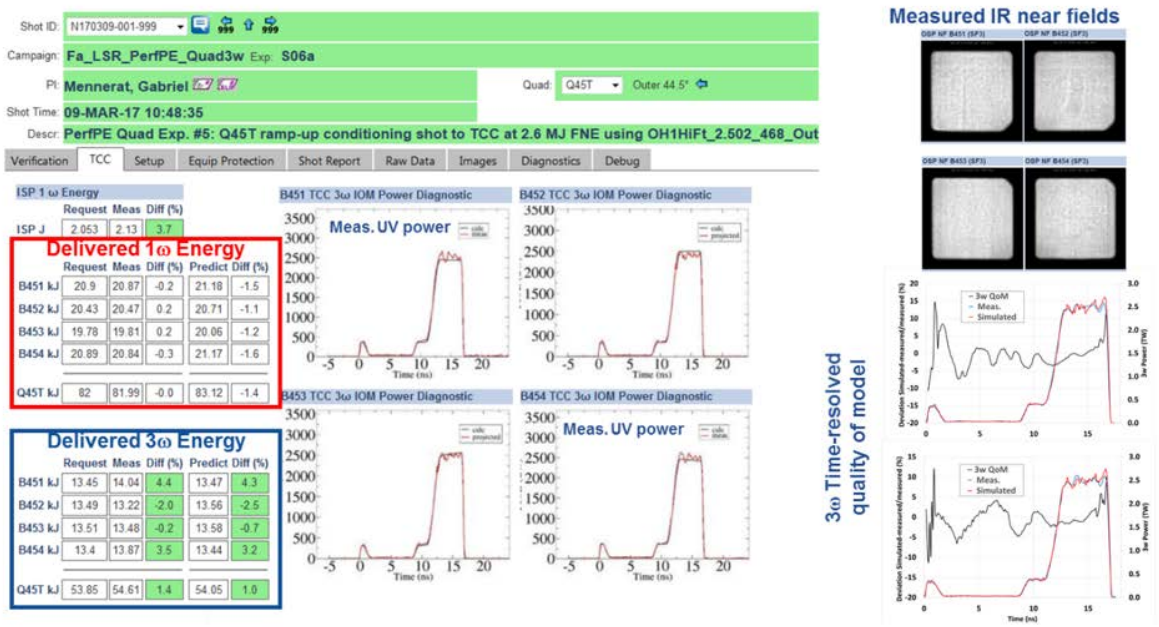

Figure 9: LPOM (Laser Performance & Operations Model) summary shot report data for N170309-001 (2.6 MJ 3ω TCC Full NIF Equivalent)

The laser diagnostics on the target chamber have a limited ability to diagnose the 3ω near-field fluence profiles at the output of the Final Optics Assembly, when appropriately configured. For this campaign, 3ω near-field data was acquired on two of the four beams in the quad. Data quality was such that it precluded accurately quantifying certain important fluence metrics like contrast, but it was sufficient to provide good quantitative information about other important metrics like flatness and edge modulation (Figure 10(a)).

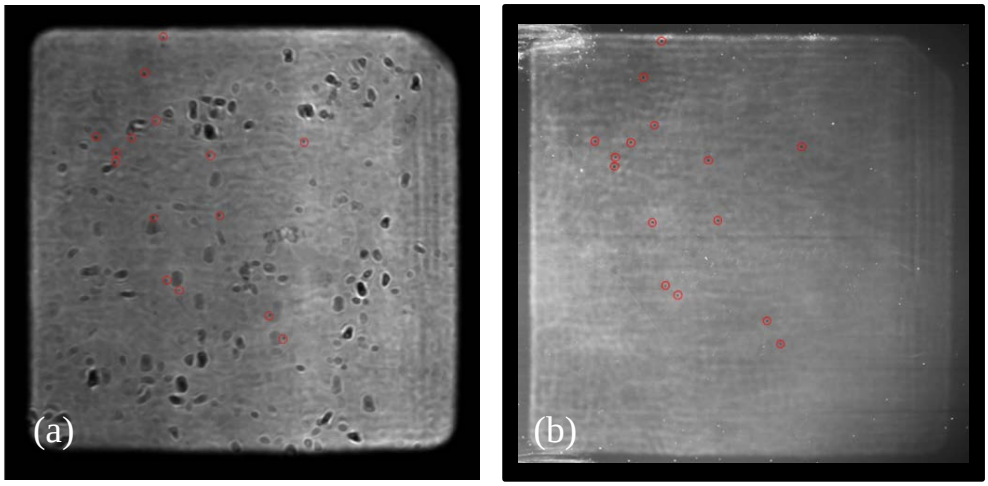

Figure 40: (a) B454 3ω near-field fluence profile measured on N170309-001-999 (2.6 MJ 3ω TCC Full NIF Equivalent). Dark obscurations are due to small localized defects in the diagnostic path. (b) Post-shot photograph of side-illuminated ADDS showing fluence-dependent damage pattern

Additional and supporting near-field fluence data was provided by the Automated Disposable Debris Shield (ADDS), the last optic in the Final Optics Assembly. Figure 10(b) shows a post-shot digital camera picture of a side-illuminated ADDS after a single high energy shot. The gray-level in the ADDS picture is approximately proportional to the quantity of light scattered from the ADDS, which is approximately

proportional to the damage density in the ADDS, which is in turn proportional to the 3ω fluence profile on the shot. Close inspection of both images reveals an identical pattern of small dark spots, identified by the red circles in the figure. The spots correspond to shadows in the high-fluence beam profile produced by damage mitigation cones machined into the up-stream wedged focus lens, confirming that 1) beam shadows and obscurations are readily recorded by the ADDS and thus 2) the majority of the dark obscurations in the diagnostic image are in the diagnostic path, not the high-fluence beam. The ADDS picture also confirms the high levels of fluence modulation at the top and left edges of the beam observed in the diagnostic data. As oriented in Figure 10, the top of the images corresponds to the thick side of the wedged focus lens where filamentation was observed.

The fluence modulation along the top of edge of the beam in Figure 10 is well-correlated with the location and quantity (~780) of filaments in the lens (S/N 271301) determined from off-line metrology. Figure 11 shows a sub-region of the fluence profile in Figure 10(a) containing the edge modulation (top left), the same sub-region thresholded to show only the area of the beam area above 15 J/cm^2 (middle left), and the density of the filaments measured in the lens (bottom left). Lineouts through the fluence regions above 15 J/cm^2 and the high-density regions of the filament map show a fair degree of correlation.

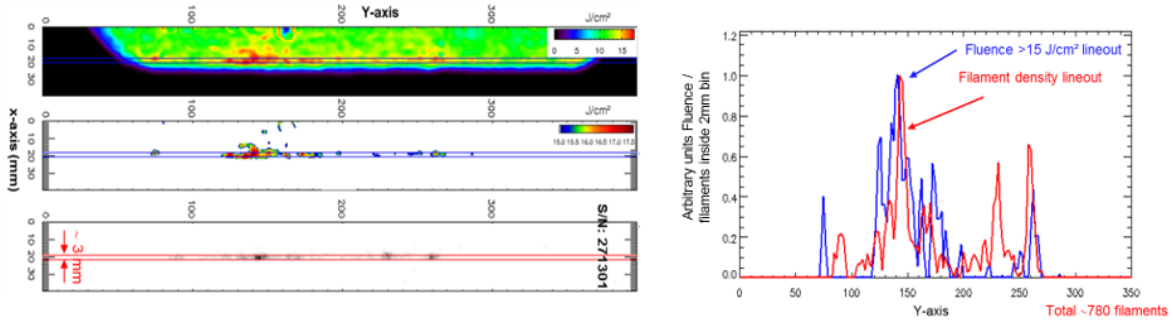

Figure 11: Close-up views of the 3ω measured fluence and filament density count (left). Fluence and filament density lineouts (right)

The level of fluence modulation from beam edge intensification observed in this campaign was not predicted by the models. To close this gap, the standard VBL model used in LPOM needed to be augmented to take full account of the B-integral accumulated at the edges of the beam in the pre-amplifier. It was also updated to include the detailed aberrations of the final optics used in the campaign. At low sigma B, the shape of the beam edge is determined by the serrated apodizer located after the regenerative amplifier and before the pre-amplifier. This apodizer is included in the standard VBL model, and in its current incarnation defines a 10%-90% edge transition width of 2.2 cm in the Main Laser.

As shown in Figure 12, the augmented VBL model is able to match the observed edge intensification fairly well, and without the need to change any of the baseline values for the nonlinear coefficients (γ) of the materials. The source of the edge intensification was confirmed by turning off the nonlinear coefficients in the model and verifying that the edge intensification was eliminated.

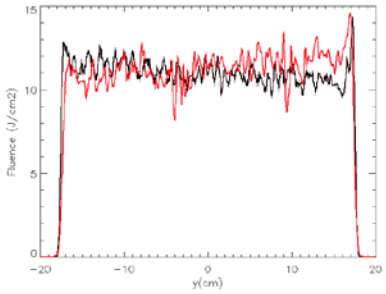

Figure 12: Average lineout 3ω fluence profiles. Measurement (red) and VBL simulation (black).

4. Future work

NIF operation at elevated energy and high sigma B is likely to require, as in the case of the spot blocker, softer beam edge apodization. Numerical simulations with VBL show that increasing the edge transition of the apodizer from 2.2 cm (current design) to 3.4 cm should mitigate the observed edge intensification (Figure 13). FY18 experiments are being planned to test this mitigation. Additional work is also being planned to confirm the values of the non-linear coefficients in the codes - particularly the off-diagonal terms used in the final optics- through focused off-line experiments.

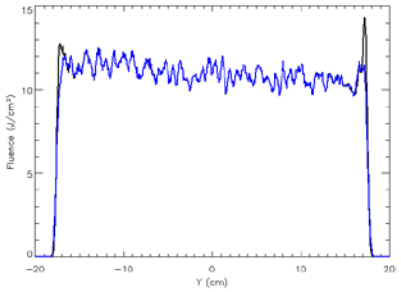

Figure 13: Average lineout 3ω fluence profiles. VBL simulation with 2.2 cm edge profile (black) and 3.6 cm edge profile (blue)

5. Appendix: Shot Table

Campaign Phase & Shot #	Beam Fate	TCC 3ω Full NIF Equiv. Energy and Power (MJ / TW)	Requested Energy (kJ per quad)	Measured Energy (kJ per quad)	Experiment number
I-1	RMDE (1ω)	1.8 / 390	61.5	63.0	N161204-002-999
I-2	RMDE (1ω)	2.0 / 410	66.6	66.8	N161206-001-999
I-3	RMDE (1ω)	2.3 / 450	75.1	75.4	N161206-002-999
I-4	RMDE (1ω)	2.5 / 470	82.9	83.4	N161208-002-999
I-5	RMDE (1ω)	2.6 / 480	86.0	86.9	N161209-001-999
I-6	RMDE (1ω)	2.2 / 430	72.3	74.5	N161211-001-999
I-7	RMDE (1ω)	2.4 / 460	78.0	79.3	N161211-002-999
I-8	RMDE (1ω)	2.6 / 480	82.2	82.7	N161212-002-999
II-1	TCC 3ω	1.8 / 390	37.3	37.2	N170212-001-999
II-2	TCC 3ω	2.0 / 410	41.5	42.2	N170219-001-999
II-3	TCC 3ω	2.3 / 450	47.6	47.2	N170224-001-999
II-4	TCC 3ω	2.5 / 470	51.8	52.4	N170307-001-999
II-5	TCC 3ω	2.6 / 480	53.9	54.6	N170309-001-999
III-1	TCC 3ω	1.1 / 230	23.1	23.7	N170401-001-999
III-2	TCC 3ω	2.6 / 480	54.0	54.4	N170402-001-999
III-3	TCC 3ω	1.1 / 230	23.1	23.6	N170402-002-999
III-4	TCC 3ω	2.5 / 470	51.9	52.8	N170402-003-999
III-5	TCC 3ω	1.1 / 230	23.1	22.5	N170402-004-999
III-6	TCC 3ω	2.5 / 470	51.9	51.9	N170403-001-999
III-7	TCC 3ω	1.1 / 230	23.1	22.8	N170403-002-999
III-8	TCC 3ω	2.5 / 470	51.9	51.6	N170403-003-999
III-9	TCC 3ω	1.1 / 230	23.1	22.1	N170403-004-999
III-10	TCC 3ω	2.5 / 470	51.9	52.4	N170403-005-999
III-11	TCC 3ω	1.1 / 230	23.1	22.4	N170404-001-999
III-12	TCC 3ω	2.5 / 470	51.9	52.1	N170402-002-999

6. Acknowledgments

The work summarized here represents the combined effort of many individuals. In particular we acknowledge the members of the NIF Power and Energy Integrated Product Team for their central role in the planning, execution, simulation, analysis, and documentation of this campaign.

This work was performed under the auspices of the U.S. Department of Energy by Lawrence Livermore National Laboratory under Contract DE-AC52-07NA27344. Lawrence Livermore National Security, LLC

7. References

[1] "NIF PE Performance Quad Phase-I: 1ω ramp-up to RMDE to 2.6 MJ FNE 3ω", 1001727654-AA (11/2016).
[2] "NIF PE Performance Quad Phase-II: 3ω ramp-up to 2.6 MJ FNE 3ω on Q45T", 1001973125-AA (02/2017).
[3] "NIF PE Performance Quad Phase-III: 3ω campaign at 2.6 MJ FNE 3ω on Q45T," 1002192461-AA (02/2017).
[4] "FY17 NIF Performance Quad Campaign: Optics damage assessment and projected optics use & cost for high-energy NIF operations", 1003081949-AA (09/2017).
[5] "Impact of quad-based beam shaping on 3ω damage rate", 1001201503-AB (05/2016).